Homoclinic orbits in a piecewise system and their relation with invariant sets

Rene O. Medrano-T.*, Murilo S. Baptista, Iberê L. Caldas

Instituto de Física, Universidade de São Paulo, C.P. 66318, CEP 05315-970 São Paulo, SP, Brazil

Abstract

Basic phenomena in chaos can be associated with homoclinic and heteroclinic orbits. In this paper, we present a general numerical method to demonstrate the existence of these orbits in piecewise-linear systems. We also show that the tangency of the stable and unstable manifolds, at the onset of the chaotic double-scroll attractor, changes the basin boundaries of two α-limit sets. These changes are evidence of homoclinicity in the dynamical system. These basins give complete information about the stable manifolds around the fixed points. We show that trajectories that depart from these boundaries (for backward integration) are bounded sets. Moreover, we also show that the unstable manifolds are geometrically similar to the existing attracting sets. In fact, when no homo- (hetero-)clinic orbits exist, the attractors are ω-limit sets of initial conditions on the unstable manifolds. © 2003 Elsevier B.V. All rights reserved.

1. Introduction

A homoclinic orbit occurs when the stable and unstable manifolds of a fixed point join. These manifolds have the following properties: trajectories departing from initial conditions on the stable manifold approach the fixed point as $t \to +\infty$; trajectories departing from initial conditions on the unstable manifold approach the fixed point as $t \to -\infty$. A manifold that forms a closed loop connecting two or more fixed points is called a *heteroclinic orbit*. There are two main difficulties to obtain homoclinic or heteroclinic orbits: both the parameter sets for which the manifolds join and the geometry of the manifolds are unknown.

It is known that the existence of homoclinic orbits is a signature of global changes in the dynamics. In two-dimensional systems studied by Andronov et al. [1], the onset of a homoclinic orbit causes the sudden appearance of periodic orbits. In the Lorenz system, homoclinic orbits can be associated with the bifurcations of a periodic set to form a chaotic set [2,3]. In the double-scroll system, the birth and changes of chaotic attractors can be related to homoclinic bifurcations [4]. For a three-dimensional class of systems, Shilnikov [5–7] showed that the existence of

---

* Corresponding author.
E-mail address: rmedrano@if.usp.br (R.O. Medrano-T.).

a homoclinic orbit may imply the existence of a horseshoe [8,9] in the neighborhood of this orbit that is responsible for the creation of a chaotic set.

A system is chaotic if it has sensitivity to initial conditions, is transitive, and has an uncountable number of periodic orbits. By Shilnikov's theorem [5–7], homoclinicity can imply the existence of a horseshoe and consequently the three conditions for chaotic motion.

However, a homoclinic orbit is structurally unstable, which means that arbitrary small parameter perturbations may destroy it and, as a consequence, also destroy its associated horseshoe. So, to better understand the role of the homoclinic orbit in the global dynamics and the existence of chaotic motion, we look for its relation with more stable sets, like attracting sets (which are different from the sets in the neighborhood of the homoclinic orbit), basins of attraction, and for specific structure of the manifolds.

We choose to work with the double-scroll circuit [10,11] because it is a piecewise system of the family for which the Shilnikov theorem applies. That is, a homoclinic orbit exists for a set of parameter ranges for which a chaotic attracting set also exists.

In general, calculating homoclinic orbits is not an easy task. In a piecewise system, we can partially determine analytically the stable and unstable subspaces containing the manifolds close to the fixed point. This can be used in a semi-analytical approach to numerically determine the homo- (hetero-)clinic orbit. In a piecewise system, the phase space is divided into domains, each with its own fixed point. Thus, it is possible to know the topology of the manifolds in each domain within a neighborhood of these points. The procedure presented here is generally applicable to any three-dimensional and piecewise-linear dynamical system.

In addition to numerically obtaining homo- (hetero-)clinic orbits, we also give conditions to numerically demonstrate the existence of a homo- (hetero-)clinic orbit to a fixed point. Furthermore, we investigate the relation of this orbit with the manifolds of the homoclinic point, the attracting set, and the basins of attraction. We also contribute to an understanding of how the presence of a homoclinic orbit changes the geometry of the trajectories, based only on the information about the subspaces. This topological description is used to describe the manifold's characteristics and topology and their relationship to the attractors. Finally, we show that the existence of a homoclinic orbit implies changes in the manifolds that result in a global change of a basin of attraction of an α-limit set.

This paper is organized as follows. In Section 2, we present the double-scroll circuit, and in Section 3, its subspaces and manifolds. In Section 4, we show how to numerically demonstrate the existence of the homo- (hetero-)clinic orbit, and in Section 5, we show the relationship between the homoclinic orbits, the manifolds, the basins of attraction, and the attractors. Finally, Section 6 contains the conclusions.

2. The double-scroll circuit

The double-scroll circuit [10,11] illustrated in Fig. 1(a) has two capacitors (C_1 and C_2), one inductor (L), a linear resistor represented by its admittance ($g = 1/R$), and a nonlinear resistor (R_N).

Fig. 1(b) shows the circuit characteristic curve: m_0 and m_1 are the slopes for the linear region, and $\pm B_p$ are the values of the V_{C_1} for which the slope changes. Applying Kirchoff's law to the circuit and changing to the dimensionless form ($x = V_{C_1}/B_p$, $y = V_{C_2}/B_p$, $z = i_L/gB_p$, $\alpha = C_1/C_2$, $\beta = C_2/Lg^2$, $\tau = gt/C_2$, $a = m_1/g$, and $b = m_0/g$) we have the circuit equations:

$$\dot{x} = \alpha[y - x - k(x)], \qquad \dot{y} = x - y + z, \qquad \dot{z} = -\beta y, \tag{1}$$

where

$$k(x) = bx + \tfrac{1}{2}(a - b)(|x + 1| - |x - 1|) \tag{2}$$

and $a = -8/7$, $b = -5/7$. Thus, the control parameters are α and β.
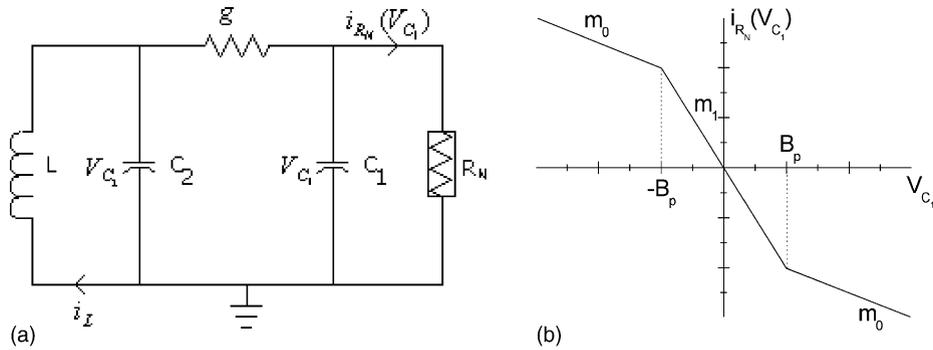
Fig. 1. (a) Schematic diagram of the double-scroll circuit. V_{C_1} and V_{C_2} are the potential across capacitors C_1 and C_2, respectively, and i_L is the current across the inductor L. (b) Characteristic curve of the nonlinear resistance R_N, showing the current i_{R_N} across R_N, with respect to V_{C_1}.

3. Subspaces of the manifolds

According to Eq. (2), we divide the domain of Eq. (1) into three parts: $D_0 = \{\mathbb{R}^3 : |x| < 1\}$, $D_+ = \{\mathbb{R}^3 : x > 1\}$, and $D_- = \{\mathbb{R}^3 : x < -1\}$. In each domain, there is a fixed point: $P_0 = (0, 0, 0)$ in D_0 and $P_\pm = (\pm\ell, 0, \mp\ell)$ in $D_\pm$, where $\ell = (b - a)/(b + 1) = 1.5$. This system has three eigenvalues in each domain. In the domains D_+ and D_-, the eigenvalues are the same.

When there is a chaotic set, one eigenvalue is real and the other two are complex conjugate. The complex eigenvalues are responsible for the two eigenvectors that determine a two-dimensional planar subspace, and the real eigenvalue is associated to the eigenvector that determines a linear subspace. In a domain around each fixed
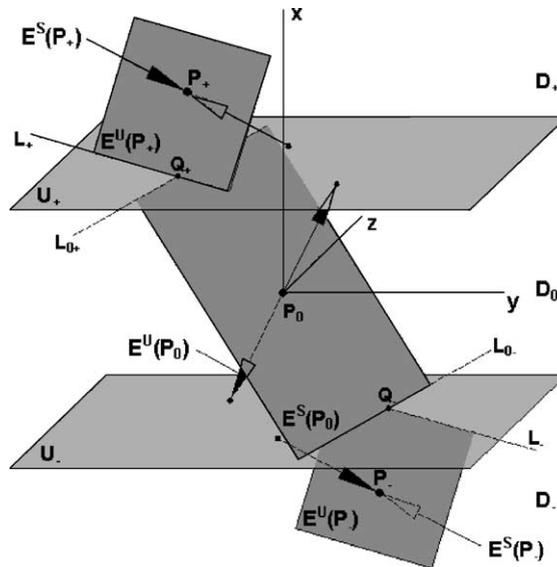
Fig. 2. Stable (E^S) and unstable (E^U) subspaces of the fixed points P_0, P_+ and P_-. The planes $U_\pm = \{\mathbb{R}^3 : x = \pm 1\}$ are the boundaries of the domains D_0 with $D_\pm$. In D_0 the unstable subspace ($E^U(P_0)$) is a line and the stable subspace ($E^S(P_0)$) is a plane. In $D_\pm$, the unstable subspace ($E^U(P_\pm)$) is a plane and the stable subspace ($E^S(P_\pm)$) is a line. The line $L_\pm$ is the intersection of $E^U(P_\pm)$ with the plane $U_\pm$. $L_{0\pm} = E^S(P_0) \cap U_\pm$ and $Q_\pm = L_\pm \cap L_{0\pm}$.

point, the manifolds W are either straight lines or surfaces and coincide with the associated linear subspace. This behavior is unlike general nonlinear systems, where subspaces and manifolds are tangent to each other only locally: in piecewise-linear systems, this tangency occurs not only in a point but in a large region of the subspace close to the fixed point. Eq. (1) is linear within the domains, and the stability of the manifolds is determined by the sign of the real part of the eigenvalues. Fig. 2 represents the subspaces of the fixed points of Eq. (1). The planes $U_\pm = \{\mathbb{R}^3 : x = \pm 1\}$ are the boundaries of the domains D_0 with $D_\pm$. In D_0, the unstable subspace ($E^U(P_0)$) is a line and the stable subspace ($E^S(P_0)$) is a plane. In $D_\pm$, the unstable subspace ($E^U(P_\pm)$) is a plane and the stable subspace ($E^S(P_\pm)$) is a line. The line $L_\pm$ is the intersection of $E^U(P_\pm)$ with the plane $U_\pm$. Notice that $L_{0\pm} = E^S(P_0) \cap U_\pm$ and $Q_\pm = L_\pm \cap L_{0\pm}$.

4. Method to obtain homo- (hetero-)clinic orbits

The problem of calculating homoclinic orbits of a fixed point requires that one find a local neighborhood around the fixed point that maps to itself for $t \to \pm\infty$. Eq. (1) has an important property: the invariant dynamics in a neighborhood of the fixed point exists only in a planar subspace and a linear subspace. Therefore, the calculation of a homoclinic orbit is reduced to the verification of the existence of a local neighborhood of the fixed point along one subspace, that, when iterated by the dynamics for $t \to \pm\infty$, approaches the neighborhood of the fixed point on the other subspace. It is clear that defining a neighborhood on the linear subspace is easier than in the planar subspace. Therefore, the calculation of a homoclinic orbit is drastically simplified: we verify the existence of a local neighborhood of the linear subspace that, when iterated by the dynamics, approaches the planar subspace for $t \to \pm\infty$.

The calculation of heteroclinic orbits is completely equivalent to that to the homoclinic orbit. However, we have to show the existence of a neighborhood of the fixed point ($P_\pm$) that goes to another ($P_\mp$) for $t \to \pm\infty$. Because Eq. (1) has odd symmetry, if the former condition is satisfied, then there exists a neighborhood of the point ($P_\mp$) that goes to ($P_\pm$) for $t = \pm\infty$.

4.1. Method to obtain homoclinic orbits

First we show how to numerically obtain the homoclinic orbit of the fixed point P_0. We determine an initial condition on the unstable subspace $E^U(P_0)$ close to P_0 (10^{-5} distant) and integrate, numerically, from this point. The resulting trajectory goes along the unstable manifold, crossing the plane U_+ at the point P_1 shown in Fig. 3. In fact, as $E^U(P_0)$ is a straight line, the point P_1 can be determined analytically. We continue integrating the trajectory until it again reaches the plane U_+ at P_2. A necessary condition for the existence of the homoclinic orbit is that $P_2 \in E^S(P_0)$, that is, the distance d between P_2 and the line L_{0+} ($=U_+ \cap E^S(P_0)$) must be zero. We regard d as positive if P_2 is between L_{0+} and P_1 and as negative if P_2 is on the other side of L_{0+}. Note that L_{0+} is an infinite line and belongs to $E^S(P_0)$. Let I be the finite interval $I \subset L_{0+}$ that is formed by $W^S(P_0) \cap L_{0+}$, where $W^S(P_0)$ is the stable manifold of P_0. When $d = 0$, P_2 belongs to $E^S(P_0)$ and, if $P_2 \in I$, there exists a homoclinic orbit. In practice, due to numerical roundoff, d is never exactly zero, and the parameters should be set such that even if $d \neq 0$ and $P_2 \notin I$, we can be sure a homoclinic orbit exists, i.e., P_2 approaches a sufficiently small neighborhood of P_0.

We can show that a homoclinic orbit exists in P_0 if we can show that there is a strip T (on the plane U_+) of size $|d| \leq \epsilon/2$, centered at L_{0+} (see Fig. 3), whose edges approach a δ neighborhood of P_0, where ϵ and δ are sufficiently small. We also need that the iteration of the strip formed by $|d| \leq \epsilon/2$ remain near P_0 for a while. Furthermore, immediately after leaving the neighborhood of P_0, iterates of the edge for which $d > 0$ (resp. $d < 0$) of the strip T go to D_+ (resp. D_-). To set P_2 as close as we want to the plane U_+, we change the integration step size to minimize the inaccuracy in the computation of P_2.
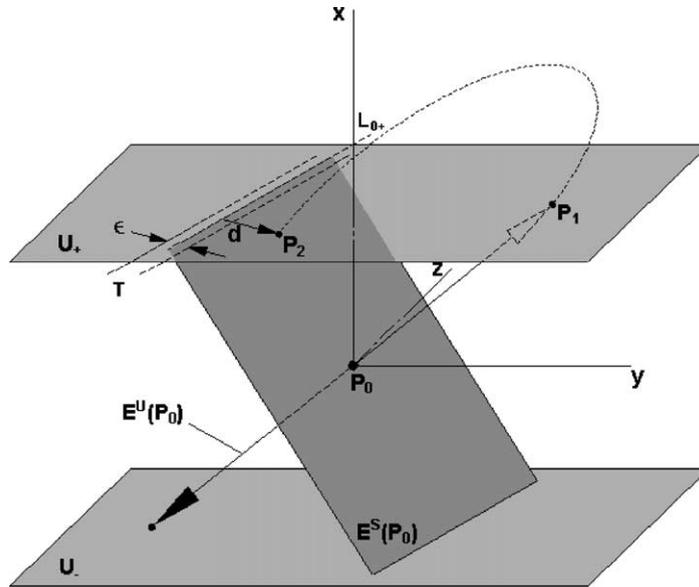
Fig. 3. Representation of the points P_1 and P_2, that are formed by $W^U(P_0) \cap U_+$. We represent the distance between L_{0+} and P_2 by d. T represents a strip of width ϵ centered at the line L_{0+}. A necessary condition for the existence of homoclinic orbits is that $d = 0$.

A homoclinic orbit exists if the following conditions are satisfied for sufficiently small values of δ and ϵ:

(I) There exist parameters α and $\Delta\alpha \in \mathbb{R}$ such that two trajectories for the parameters α and $\alpha + \Delta\alpha$ (or $\alpha - \Delta\alpha$), departing from the neighborhood of P_0, remain ϵ close to each other until they reach the point P_2.

(II) The parameters α and $\Delta\alpha$ are such that $P_2(\alpha)$ is positioned on the strip T at $d > 0$ and $P_2(\alpha + \Delta\alpha)$ (or $P_2(\alpha - \Delta\alpha)$) at $d < 0$, for $|d| \leq \epsilon/2$.
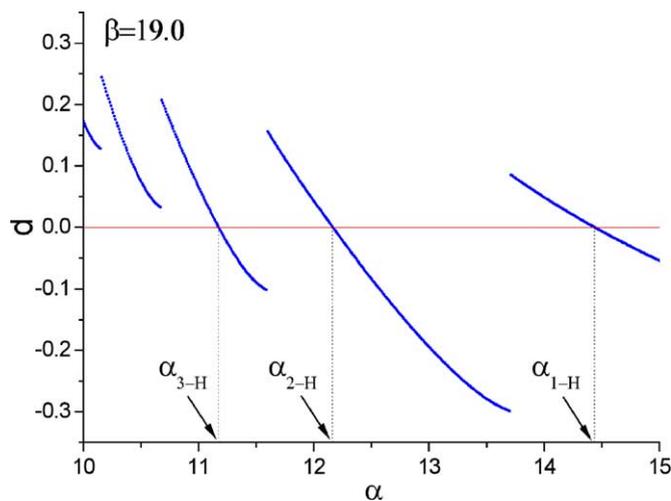
Fig. 4. The distance d with respect to the parameter α, for a fixed parameter $\beta = 19.0$. Homoclinic orbits appear for α values for which $d = 0$, including the three values indicated: α_{3-H}, α_{2-H}, and α_{1-H}.
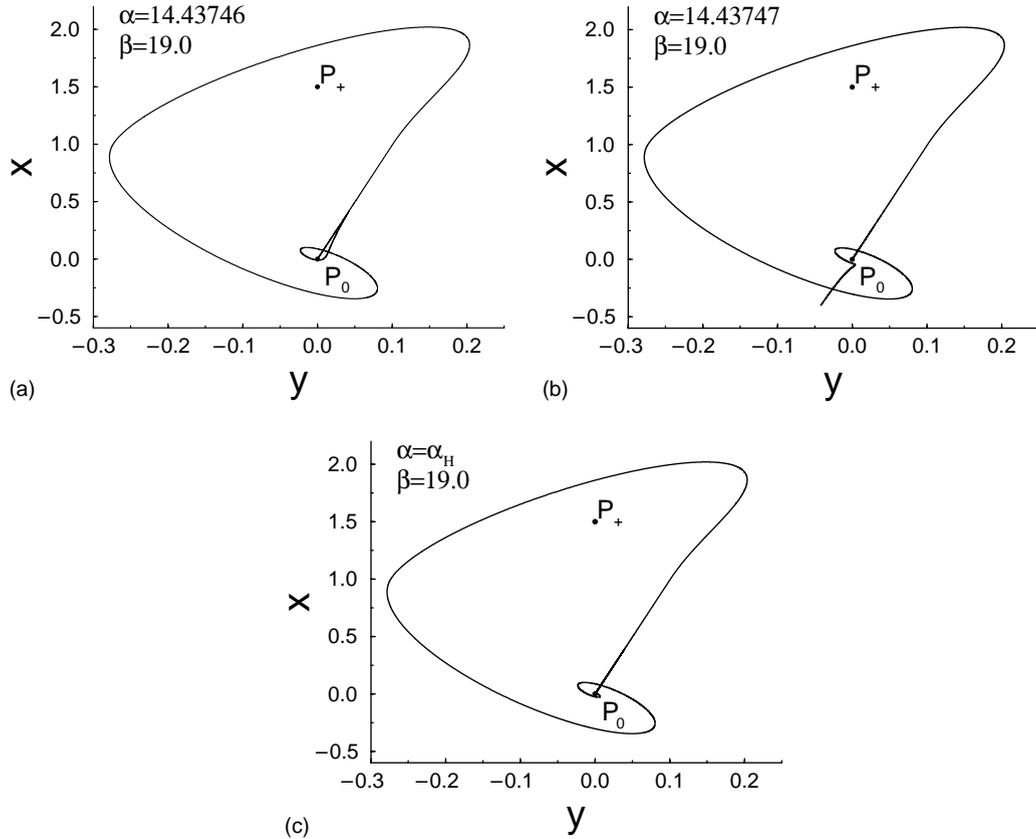
Fig. 5. A trajectory departing from the vicinity of P_0 on $E^{\mathrm{U}}(P_0)$, for the parameter: (a) $\alpha < \alpha_H$; (b) $\alpha > \alpha_H$; and (c) $\alpha = \alpha_H$. Here $\alpha_H = 14.43746643008159$ is the parameter for which an orbit homoclinic to P_0 exists. In (a), this trajectory leaves $E^{\mathrm{U}}(P_0)$ and returns to the neighborhood of P_0, heading up toward the plane U_+. In (b), the contrary happens, i.e., this trajectory leaves $E^{\mathrm{U}}(P_0)$ and returns to the neighborhood of P_0, but heading down toward the plane U_+. In (c) this trajectory leaves P_0 and returns to it.

(III) There is a parameter $\alpha' \in [\alpha, \alpha + \Delta\alpha]$ (or $\alpha' \in [\alpha, \alpha - \Delta\alpha]$) such that the trajectory departing from $P_2(\alpha')$ reaches a δ neighborhood of P_0 and goes to D_+ for $t \to +\infty$. There is also $\Delta\alpha' \in \mathbb{R}$ such that $P_2(\alpha' + \Delta\alpha')$ (or $P_2(\alpha' - \Delta\alpha')$) goes to D_- for $t \to +\infty$.

(IV) $|\alpha' - \alpha_H| \ll |\alpha - \alpha_H|$ and $\Delta\alpha' \ll \Delta\alpha$, where α_H is the value of α that exactly yields a homoclinic orbit.

If conditions I–IV are satisfied, we conclude that a homoclinic orbit exists for α_H in the interval $[\alpha', \alpha' + \Delta\alpha']$ (or $[\alpha', \alpha' - \Delta\alpha']$).

Condition II is a rough tuning of the parameter α that lets us estimate the parameter α', and condition III is a fine tuning of the parameter α that lets us estimate the parameter α_H. While $\Delta\alpha$ is of the order of 10^{-3}, $\Delta\alpha'$ is of the order of 10^{-15}. We take the value of α' as α_H. To estimate the maximum size of $\Delta\alpha$, we study how d changes as we vary α (Fig. 4) and verify that for $\Delta\alpha < 10^{-2}$, $\epsilon < 10^{-8}$, and therefore $|d|$ is very small. Condition III is based on the fact that the homoclinic orbit is not structurally stable, that is, arbitrarily small variations of α_H change completely the behavior of the trajectory departing from P_2. This structural instability is illustrated in Fig. 5. For $\alpha < \alpha_H$ (Fig. 5(a)), we have $d > 0$ and the divergence is in the direction of D_+; for $\alpha > \alpha_H$, we have $d < 0$ and divergence in the direction of D_- (Fig. 5(b)). Fig. 5(c) shows the case $\alpha = \alpha' = \alpha_H$.
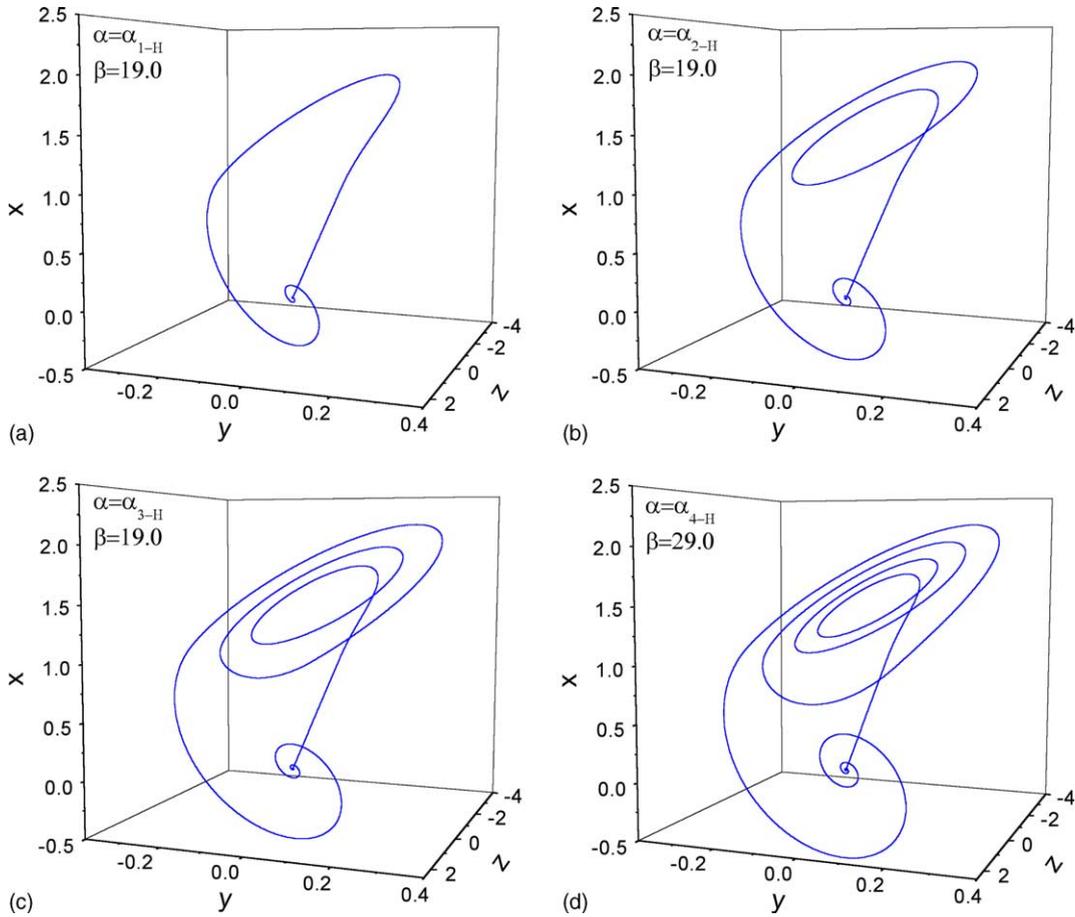
Fig. 6. Homoclinic orbits of the point P_0 for four values of the parameters α and β: (a) $\alpha_{1-H} = 14.43746643008159$ and $\beta = 19.0$; (b) $\alpha_{2-H} = 12.165457244219103$ and $\beta = 19.0$; (c) $\alpha_{3-H} = 11.174540527682883$ and $\beta = 19.0$; (d) $\alpha_{4-H} = 14.85399064174358$ and $\beta = 29.0$.

Another reason why we have to consider $d \neq 0$ and $\Delta\alpha' \neq 0$ is that we cannot work with infinities. The "exact" homoclinic orbit needs an infinite time to return to P_0, and the associated parameters cannot be specified with infinite precision. Instead, we regard our numerical calculations as being a satisfactory approximation to the homoclinic orbit when conditions I–IV are satisfied and $\delta \leq 10^{-5}$, i.e., the trajectory of P_2 gets at least 10^{-5} close to the fixed point P_0. The orbit of Fig. 5(c) is the $1 - H$ family, because it turns one time around the fixed point P_+. For the same β, there may exist other homoclinic orbits of the same type, and the same method presented here can be applied to locate these other $n - H$ families (i.e., those that turn n times around P_+). We just need to consider P_2 as the crossing of the trajectory departing from P_0 after n turns around the point P_+. In Fig. 6, we show the $1 - H$, $2 - H$, $3 - H$, and $4 - H$ homoclinic orbits. For each homoclinic orbit family in P_0 presented here, there is another symmetrically opposite, with a looping around P_-, with the same parameters. To see this, we just need to change the initial condition close to P_0 to the other side of the unstable subspace.

The procedure described in this section is applicable when the real eigenvalue λ and the real part of the complex eigenvalue ρ are of the same order. In this case ($\beta = 19.0$ and $\alpha = [10.0, 15.0]$), the ratio $|\lambda/\rho|$ is in the interval $[2.4, 2.9]$. When the fixed point has a linear stable subspace and a planar unstable subspace, we integrate the system
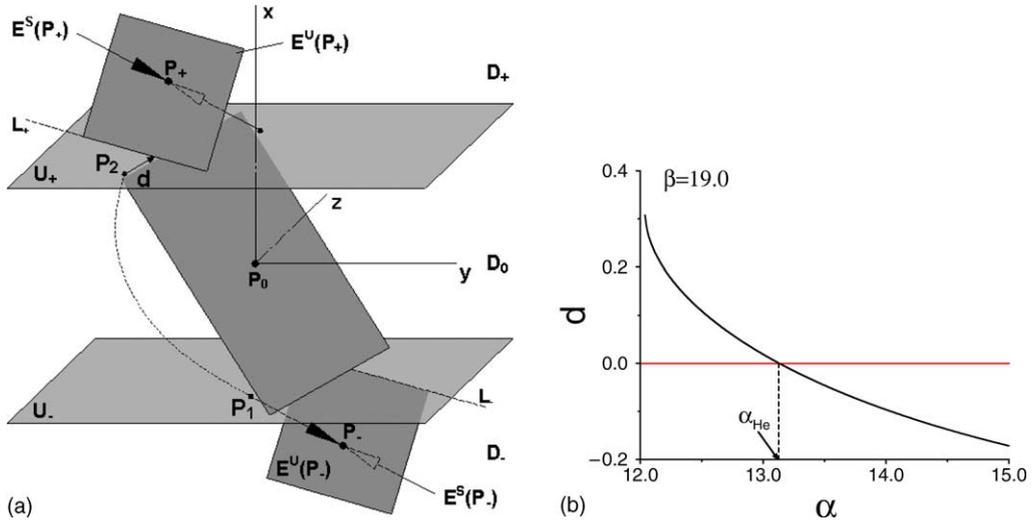
Fig. 7. (a) Representation of the points P_1 and P_2 that are formed by $W^S(P_-) \cap U_-$ and $W^S(P_-) \cap U_+$, respectively, and the distance d between the point P_2 and the line L_+, on U_+. A heteroclinic orbit exists connecting the points P_+ to P_-, if $d = 0$. (b) For a fixed $\beta = 19.0$, we show the distance d with respect to the parameter α.

backward in time, using the initial condition along the stable manifold. This is the method used to determine homoclinic orbits to the points P_+ or P_-. Next, we describe the method to calculate heteroclinic orbits which can also be used to calculate homoclinic orbits when the ratio $|\lambda/\rho| \gg 1$.

4.2. Method to obtain heteroclinic orbits

The heteroclinic orbit is the orbit that joins two or more fixed points in the phase space. The unstable manifold of the first fixed point joins the stable manifold of another fixed point, and its unstable manifold joins the stable manifold of the next fixed point, and so on, until the unstable manifold of the last fixed point joins the stable manifold of the first point. In this section, we show that conditions I–IV are sufficient to demonstrate that a heteroclinic orbit exists around the P_+ and P_- fixed points. We integrate the system backward in time with an initial condition on the stable manifold of P_- and minimize the distance d (Fig. 7(a)), fixing β and changing α by $\Delta\alpha$ to obtain $d \leq \epsilon/2$ (Fig. 7(b)). Then we refine the approach of P_2 to P_+, by finding α' such that the trajectory of P_2, for a backward time integration, converges to a δ neighborhood of P_+. Due to the odd symmetry of Eq. (1), the unstable manifold of P_+ is connected to the stable manifold of P_-, and therefore the heteroclinic orbit should exist for $\alpha = \alpha' = \alpha_H$.

If one wants to see a heteroclinic orbit, one has to be careful with the ratio $|\lambda/\rho|$ defined in Section 4.1 for the eigenvalues. Although conditions I–IV specify the existence of a heteroclinic orbit, its visualization depends on the ratio $|\lambda/\rho|$. If $|\lambda/\rho| \approx 1$, then the heteroclinic orbit is just the trajectory of P_-, under backward time integration, along the stable manifold together with the trajectory leaving the other direction of the stable manifold connecting P_+. But, as in the general case, the ratio $|\lambda/\rho|$ at the fixed points P_+ and P_- ($\beta = 19.0$ and $\alpha = [10.0, 15.0]$) is within the interval [14.8, 28.2]. In other words, the modulus of the real eigenvalue λ associated to the stable manifold $E^S(P_\pm)$ is much larger than the real part of the complex eigenvalues ρ. This implies that when a trajectory is integrated backward in time from P_-, it approaches the fixed point P_+ only for a brief time before diverging quickly from a neighborhood of P_+. In this case, we must modify the above procedure to visualize the heteroclinic orbit.
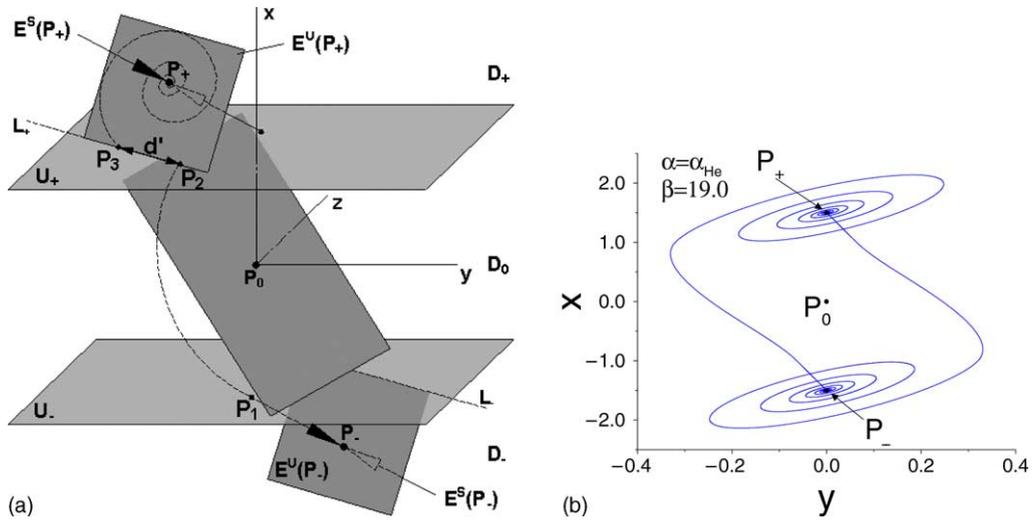
Fig. 8. For the parameters $\alpha_{He} = 13.1326237991123528$ and $\beta = 19.0$ there is a heteroclinic orbit connecting P_+ to P_-. The orbit connecting the points P_1 and P_2, shown in (a) (which are the same points represented in Fig. 7(a)) can be numerically determined. To visualize this heteroclinic orbit, an initial condition close to $P+$, on the plane $E^U(P_+)$, must be chosen such that an orbit leaving from it, for forward iteration, crosses the plane U_+ at the point P_3 and the distance d' between P_3 and P_2 is zero. (b) The heteroclinic orbit.

After finding the parameter interval $\alpha' \pm \Delta\alpha'$ for which a heteroclinic orbit exists, we find an initial condition, δ' close to the point P_+, that, when integrated by a positive time, approaches a d' neighborhood of the point P_2. More specifically, we determine a circle of initial conditions, centered at P_+ with radius δ' on the $E^U(P_+)$ plane, and integrate these points for a positive time until their trajectories cross L_+ at P_3 (Fig. 8(a)). Then we calculate the distance d' between P_3 and P_2 (Fig. 8(a)). We consider the trajectory that leaves a δ' neighborhood of P_+ and reaches L_+ with the minimum d', which is very small, as a good approximation to the heteroclinic orbit. In Fig. 8(b), we show a heteroclinic orbit connecting P_- with P_+. The same procedure is used to obtain the homoclinic orbit to P_+ (Fig. 9(a)) and one of the family $25 - H$ (Fig. 9(b)).
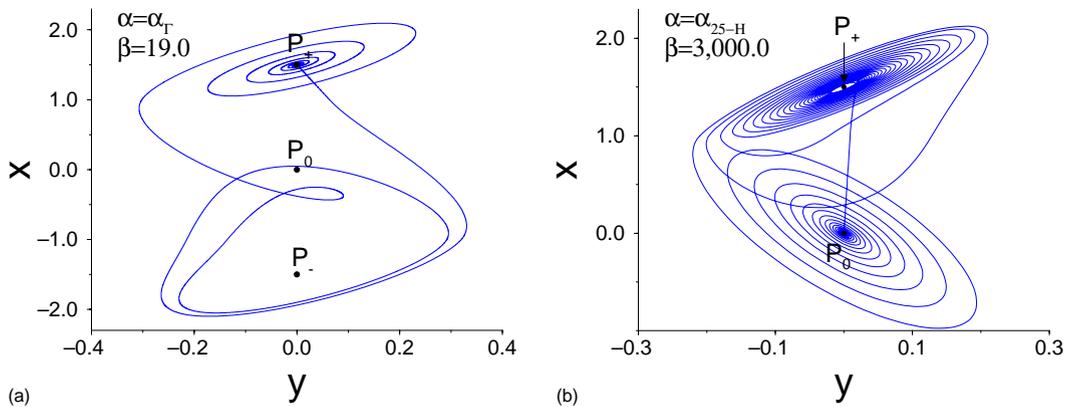
Fig. 9. (a) Homoclinic orbit of the point P_+ for the parameters $\alpha_\Gamma = 13.1251380866$ and $\beta = 19.0$. (b) A homoclinic orbit of P_0 for the parameters $\alpha_{25-H} = 376.95172431$ and $\beta = 3000$. Note that this homoclinic orbit, before returning to P_0, turns 25 times around the point P_+.

5. Manifolds, chaotic attractors and basins of attraction

The double-scroll system has two types of chaotic attractors, known as the "Rössler-type" attractor (Fig. 10(a)) and the "double-scroll" attractor (Fig. 10(b)). Here we discuss how these chaotic attractors are related to the subspaces of the fixed points and the manifolds introduced in this work. Because the manifolds' geometry, close to the fixed points, is completely described by a subspace of lower dimension, an understanding of the subspace structures can describe the geometry of the manifolds and the attractors. Our main goal is to understand how the presence of a homoclinic orbit changes the global geometry of the trajectories, based only on the information about the subspaces. This topological description will be used to describe the manifold characteristics and topology and their relations with the mentioned chaotic attractors. Finally, we will show that the existence of a homoclinic orbit implies changes in the manifolds, which results in a global change of a basin of attraction of the α-limit set of $W^{S}(P_0)$.

5.1. Chaotic attractors

When Eq. (1) has a chaotic attractor, the modulus of the real eigenvalue is much bigger than the real part of the complex eigenvalues. In the domain D_0, the real eigenvalue (whose eigenvectors form the subspace of P_0) is associated with the unstable subspace. Therefore, the trajectory quickly leaves this domain. In the domains D_+ and D_-, the real eigenvalues are associated with the stable subspace of P_+ and P_-. Therefore, the trajectory converges quickly to the vicinity of the unstable subspace of P_+, or P_-, which are planes. Most of the time, the trajectory is out of the domain D_0. Let us take an initial condition near the unstable subspace of P_0 ($E^{U}(P_0)$) with $0 < x < 1$. The trajectory goes to D_+ along this subspace and approaches the stable subspace of P_+, $E^{S}(P_+)$. As the trajectory cannot cross the unstable subspace $E^{U}(P_+)$, it spirals, going exponentially away from P_+, getting even closer to $E^{S}(P_0)$, until it crosses the boundary U_+. If it crosses on the right side of L_+ ($d > 0$), the trajectory is attracted again to the vicinity of P_+, and the Rössler attractor is formed. For a larger α value, the trajectory can cross the boundary L_+ on the left side ($d < 0$), where it is attracted to P_0 by the stable subspace $E^{S}(P_0)$ and quickly goes to the domain D_- by the effect of $E^{U}(P_0)$. Then, it is attracted to P_- by the stable subspace ($E^{S}(P_-)$) until it approaches the unstable subspace ($E^{U}(P_-)$). Thus, the same phenomenon as previously described around P_+ occurs, and the double-scroll attractor is formed.
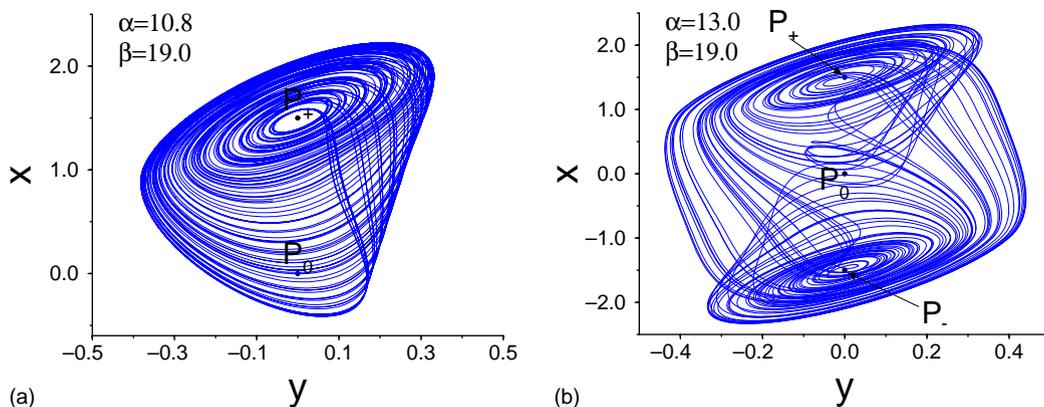
Fig. 10. Two chaotic attractors of the double-scroll system: (a) the Rössler-type attractor for the parameters $\alpha = 10.8$ and $\beta = 19.0$; (b) the double-scroll attractor for $\alpha = 13.0$ and $\beta = 19.0$.
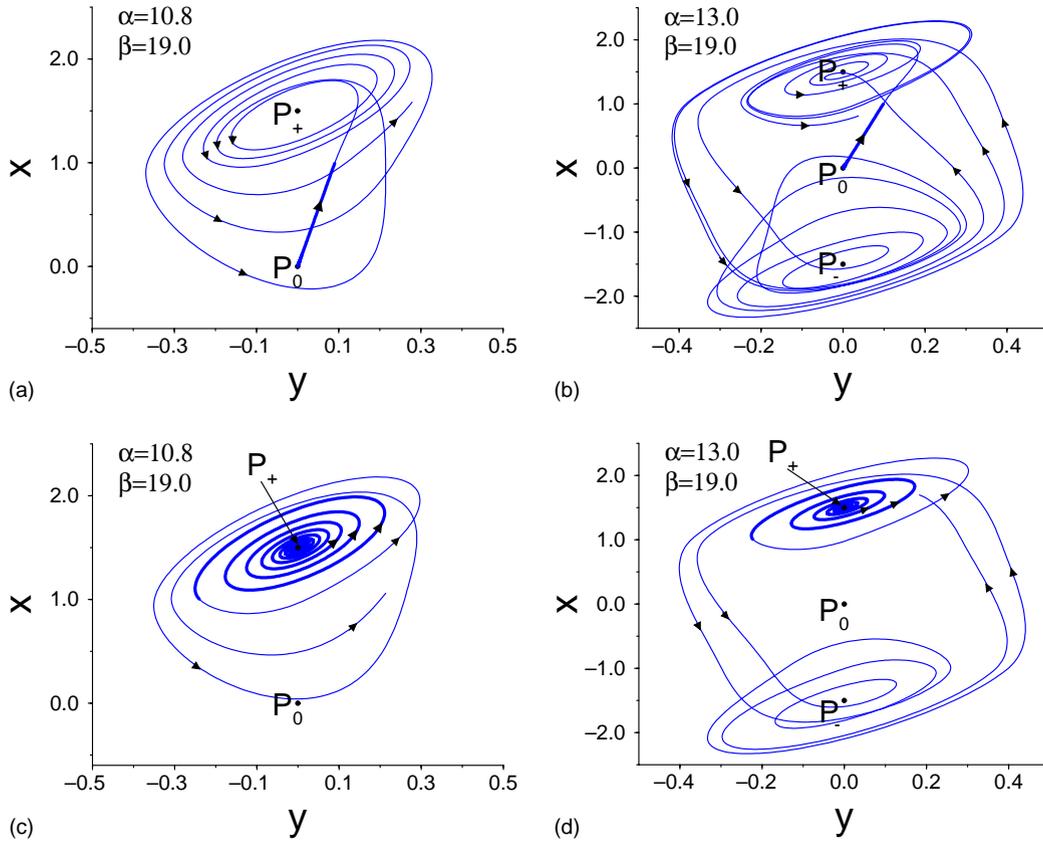
Fig. 11. (a) The one-dimensional unstable manifold $W^U(P_0)$ for the parameters $\alpha = 10.8$ and $\beta = 19.0$, where the system presents the Rössler-type attractor. (b) $W^U(P_0)$ for the parameters $\alpha = 13$ and $\beta = 19.0$, where the system presents the double-scroll attractor. For these parameter sets, no homo- (hetero-)clinic orbits exist. The fact that the manifolds are geometrically similar to the attracting sets shown in Fig. 10 means that the attractors belong to the closure of the unstable manifold $W^U(P_0)$. The thick orbits represent $E^U(P_0)$. (c) and (d) are for the same parameters as (a) and (b), respectively, but show a trajectory on the unstable manifold of P_+. Again, the attracting sets belong to the closure of the unstable manifold $W^U(P_+)$. The thick trajectories belong to unstable subspace $E^U(P_+)$.

5.2. Unstable manifold

In Fig. 11(a) and (b), we show that the topology of the one-dimensional unstable manifold $W^U(P_0)$ is equivalent to that of the attractor, that is, trajectories departing from initial conditions on $W^U(P_0)$, in the vicinity of P_0, have the same geometry of the attractor shown in Fig. 10(a). These figures are done for a parameter set for which a Rössler-type and a double-scroll attractor exist, respectively, and there are no homo- (hetero-)clinic orbits. Similar results hold for $W^U(P_\pm)$ (Fig. 11(c) and (d)). Hence, the attractors of the double-scroll system are ω-limit sets of initial conditions on the unstable manifolds W^U. When there is a homo- (hetero-)clinic orbit, any trajectory departing from W^U converges to a fixed point instead of converging to the attractor. Therefore, the ω-limit set of initial conditions on $W^U(P_0)$ is the fixed point P_0 when a homoclinic orbit exists.

5.3. Stable manifold

All initial conditions on the stable manifold converge to the fixed point as $t \to +\infty$. On the other hand, initial conditions on the stable manifold of P_0 converge to two different places as $t \to -\infty$: either these initial conditions
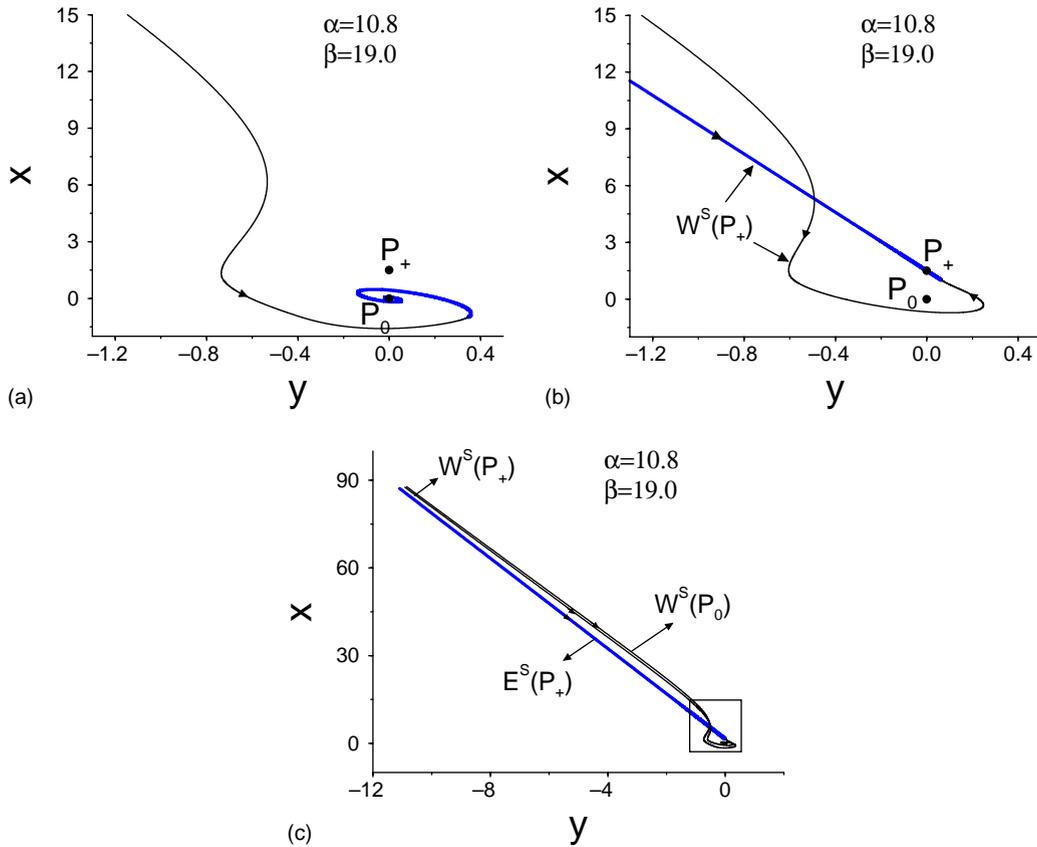
Fig. 12. (a) Orbit belonging to $W^S(P_0)$. (b) A portion of $W^S(P_+)$ in the neighborhood of P_+. The superior part of $W^S(P_+)$ (thick line in (b)) is a straight line that extends towards the point $(x, y, z) = (+\infty, -\infty, -\infty)$. (c) The orbit that belongs to $W^S(P_0)$ and part of the manifold of $W^S(P_+)$, for a large region of the phase space. The purpose of this figure is to assure that initial conditions on $W^S(P_0)$ tend to $x_{+\infty}$ along the stable subspace $E^S(P_+)$ as $t \to -\infty$.

go to $x = +\infty$ (also $y = z = -\infty$) or to $x = -\infty$ (also $y = z = +\infty$). We denote by $x_{+\infty}$ the α-limit set of initial conditions in $W^S(P_0)$ that go to $x = +\infty$. Analogously, we denote by $x_{-\infty}$ the α-limit set of initial conditions in $W^S(P_0)$ that go to $x = -\infty$. To clarify this, in Fig. 12(a), we show an orbit belonging to $W^S(P_0)$ in the neighborhood of P_0, and in Fig. 12(b), a piece of $W^S(P_+)$ in the neighborhood of P_+. Note that the superior part of $W^S(P_+)$ (thick line in Fig. 12(b)) is a straight line, which we know extends toward the set $x_{+\infty}$. In Fig. 12(c), we show the orbit that belongs to $W^S(P_0)$ and part of the manifold of $W^S(P_+)$ for a large region of the phase space. The purpose of this figure is to assure that initial conditions on $W^S(P_0)$ tend to $x_{+\infty}$ along $E^S(P_+)$. Since the double-scroll system has odd symmetry, the same geometry is observed for the stable manifolds of $W^S(P_0)$ and $W^S(P_-)$. Hence, initial conditions on $W^S(P_0)$ go to $x_{-\infty}$. Thus, it is convenient to treat $W^S(P_0)$ as two separated subsets that define the initial conditions that go either to $x_{+\infty}$ or $x_{-\infty}$. Note that the branch of $W^S(P_+)$ shown in Fig. 12(b) coincides with $E^S(P_+)$ shown in Fig. 12(c).

To visualize the α-limit sets $x_{+\infty}$ and $x_{-\infty}$, we show in Fig. 13(a) the behavior of trajectories departing from the neighborhood of P_0 for backward time integration. In this figure, the dark points in the vicinity of P_0 are the initial conditions that go to $x_{+\infty}$ around $E^S(P_+)$ (points on the top left of Fig. 13(a)), for an arbitrary negative time. Gray points in the vicinity of P_0 are the initial conditions that go to $x_{-\infty}$ around $E^S(P_-)$ (points on the bottom right of
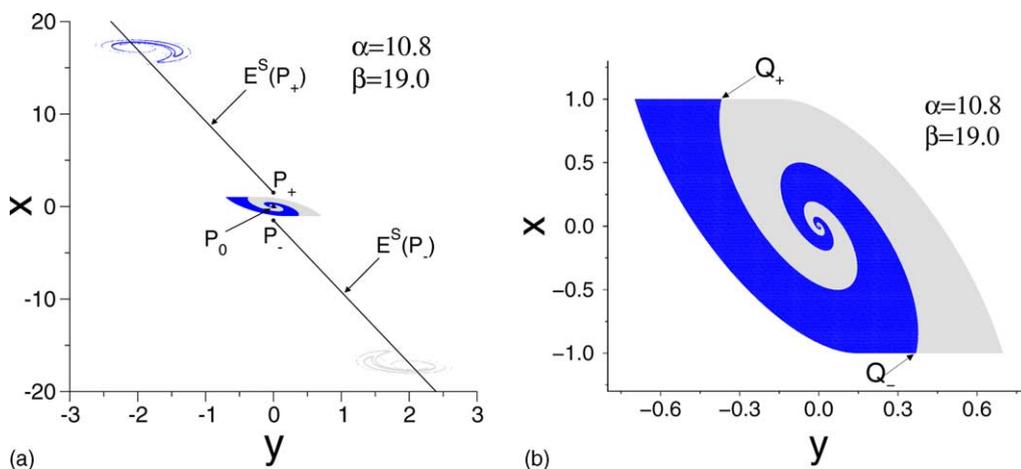
Fig. 13. (a) Trajectories departing from the neighborhood of P_0 for backward integration. The dark points in the vicinity of P_0 go to $x > 0$ (points on the top left) for a negative time. Gray points in the vicinity of P_0 go to $x < 0$ (points on the bottom right), for this same negative time interval. (b) Magnification of (a) for points for which $W^S(P_0) \cap E^S(P_0) \neq \emptyset$.

Fig. 13(a)), for this same negative time. In Fig. 13(b), we show a magnification of Fig. 13(a) for points for which $W^S(P_0) \cap E^S(P_0) \neq \emptyset$. Note that the branch of $E^S(P_+)$ shown in Fig. 13(a) coincides with a branch of $W^S(P_+)$ shown in Fig. 12(b). The same happens for P_-.

This manifold property can be explored to understand its geometry in the vicinity of the homoclinic point. The points in $W^S(P_0) \cap E^S(P_0)$ form the basin of attraction of the α-limit sets $x_{\pm\infty}$. In the basin shown in Fig. 13(b), there are two boundaries where the black color meets the gray color. These boundaries do not belong to the basin of either of the α-limit sets $x_{+\infty}$ and $x_{-\infty}$. Therefore, the α-limit set of these boundaries should be a bounded set.

In Fig. 13(b), we indicate the points $Q_{\pm}$ that lie in the vicinity of a homoclinic orbit, if one exists (see also Fig. 2). Although the points $Q_{\pm}$ seem to be close to the basin boundaries of $x_{\pm\infty}$, they are not part of the boundaries. These points belong to $E^U(P_+)$ and do not belong to $W^U(P_+)$. A trajectory leaving $Q_{\pm}$, for backward integration, does not go to the point P_+ and does not belong to a homoclinic orbit.

5.4. Homoclinic orbits, the double-scroll attractor, and the basins of attraction

When the parameters in Eq. (1) are such that the double-scroll attractor exists, the basin boundary of the sets $x_{\pm\infty}$ becomes more complex than in the case of the Rössler attractors. Four more boundaries appear. Again, these boundaries belong to trajectories that should asymptotically go to bounded sets for backward time integration. In Fig. 14(a), we show the basin of the limit sets $x_{\pm\infty}$ and a homoclinic orbit. A magnification of this figure in the region of the point Q_+ is shown in Fig. 14(b). We see a homoclinic orbit passing along a new basin boundary created by the presence of the double-scroll attractor. This new basin boundary, a gray strip in this figure, can be better visualized in Fig. 14(c), where we have omitted the homoclinic orbit.

This new gray strip appears due to the existence of the double-scroll attractor, and it is a consequence of the fact that the manifolds $W^S(P_0)$ and $W^U(P_0)$ are becoming tangent. The approach of these two manifolds is responsible for two new bounded trajectories departing from P_0 in backward time. In addition, a special case of a bounded trajectory is about to be created: a trajectory that leaves P_0, and for $t \to -\infty$ returns to P_0, i.e., the homoclinic orbit. The existence of a homoclinic orbit (Fig. 14(a)) to the point P_0 means that two trajectories, departing from P_0 for backward integration, leave $E^S(P_0)$ and do not go any longer to the limit sets $x_{\pm\infty}$. Instead, they bounce back and
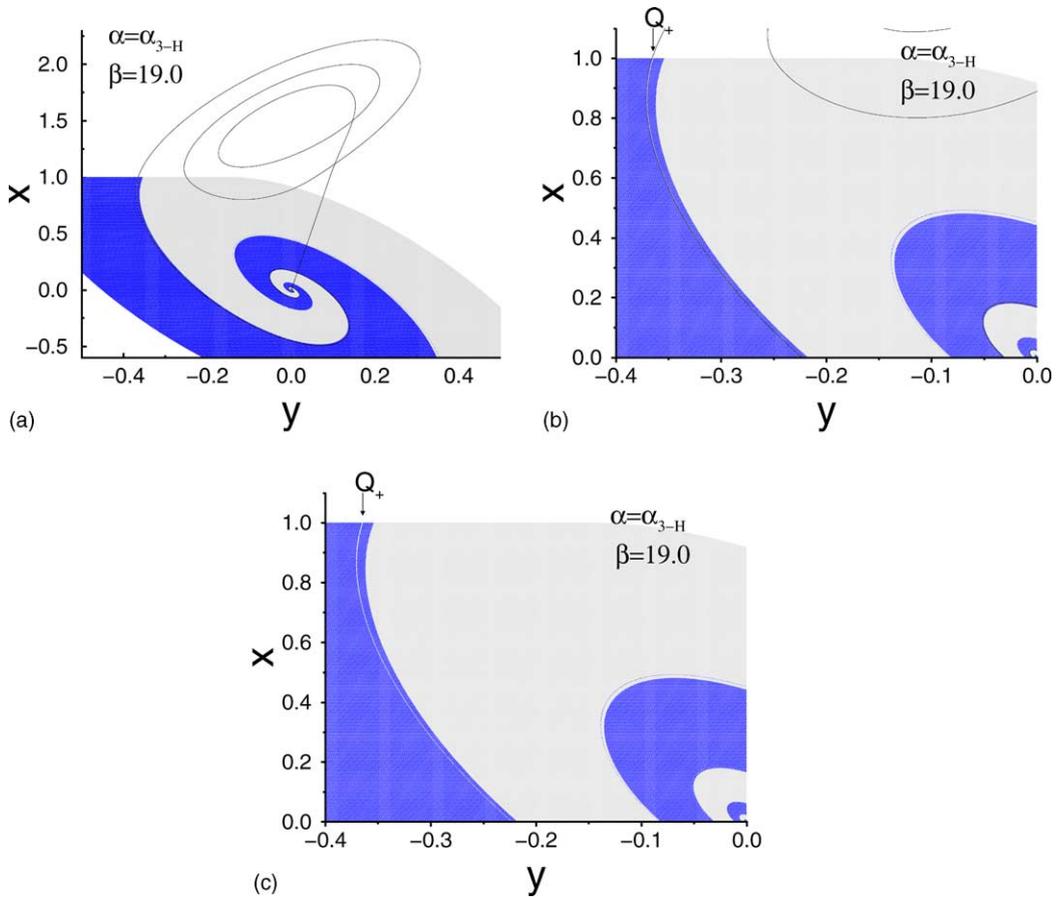
Fig. 14. (a) The basin of the α-limit sets $x_{\pm\infty}$ and a homoclinic orbit for the parameters $\alpha_{3-H} = 11.174540527682883$ and $\beta = 19.0$. (b) Magnification of (a) in the region of the point Q_+. A homoclinic orbit passes along the basin boundary of the sets $x_{\pm\infty}$. This basin boundary, a gray strip in this figure, can be better visualized in (c), where we do not show the homoclinic orbit.

return to P_0 along its one-dimensional unstable subspace, $E^U(P_0)$. In fact, we believe that these new boundaries (on $E^S(P_0)$) belong to the homoclinic orbit. So a trajectory leaving the point P_0 along $E^U(P_0)$ enters $E^S(P_0)$ along the boundaries of the limit sets $x_{\pm\infty}$.

   We believe the other four non-trivial trajectories, which belong to the boundaries of the $\pm\infty$ attractor, go to an unstable chaotic set within the domain D_0 in backward time.

6. Conclusions

   We propose a series of conditions to demonstrate the existence of homoclinic and heteroclinic orbits in piecewise-linear systems. Satisfying these conditions implies the existence of a parameter within a specified range for which those special orbits must exist. We apply these conditions to obtain homo- and heteroclinic orbits for the three fixed points of the double-scroll system. We show examples of homoclinic orbits to the fixed point P_0 in the central domain and of a heteroclinic orbit connecting P_+ and P_-, the other fixed points in the external domains. Once the proposed conditions are constructed based on properties of the system for a finite range of parameter values, they can

instruct an experimentalist who seeks the existence of homo- (hetero-)clinic orbits in piecewise-linear laboratory systems whose parameters cannot be maintained with infinite precision.

We also give a full geometrical picture of the stable manifolds of the point P_0. We describe a basin of attraction, located on the subspace $E^S(P_0)$, of two important α-limit sets, one called $x_{+\infty}$, located at $(x, y, z) = (+\infty, -\infty, -\infty)$ and another called $x_{-\infty}$, located at $(x, y, z) = (-\infty, +\infty, +\infty)$. To understand the geometry of the stable manifold $W^S(P_0)$, we must understand the geometry of this basin of attraction. This basin, formed by two subsets, represents points that go either to $x_{+\infty}$ or to $x_{-\infty}$. The boundary between these two subsets belongs to trajectories that, for backward integration, do not go to either α-limit set. Therefore, trajectories departing from this boundary should evolve to a different, bounded α-limit set.

Changes in the manifolds, which indicate that a homoclinic orbit exists, can be observed by looking at the changes in this basin. For parameters within the range for which the double-scroll attractor exists, the basin of the limit sets $x_{\pm\infty}$ has six continuous boundaries, four more boundaries than when a Rössler-type attractor exists. These extra boundaries are a consequence of the complexity of basin of attraction and result from the imminent tangency between the stable and unstable manifolds of P_0. At the tangency, one special bounded orbit is created that connects P_0 to itself, which is the homoclinic orbit. Therefore, the creation of the double-scroll attractor enables the existence of the homoclinic orbit. We believe this new boundary belongs to the homoclinic orbit.

As a way to understand the relation between the invariant manifolds and the attracting set, we show that the attractors are ω-limit sets of initial conditions on the manifolds W^U, when no homo- (hetero-)clinic orbits are present. Otherwise, when there are homo- (hetero-)clinic orbits, there are two ω-limit sets of initial conditions on W^U: one is the attractor, and the other is a fixed point.

Acknowledgements

References

[1] Andronov, Leontovich, Gordon, Maier, Israel Program of Scientific Translation, Jerusalem, 1971.
[2] J. Kaplan, J. Yorke, Commun. Math. Phys. 67 (1979) 93–108.
[3] J. Yorke, E. Yorke, J. Stat. Phys. 21 (1979) 263–278.
[4] S. Kahan, A.C. Sicardi-Schifino, Physica A 262 (1999) 144–152.
[5] L. Shilnikov, Sov. Math. Dokl. 6 (1965) 163–165.
[6] L. Shilnikov, Math. USRR Sbornik 6 (1968) 427–438.
[7] L. Shilnikov, Math. USRR Sbornik 10 (1970) 91–102.
[8] S. Smale, Differential and Combinatorial Topology, Princeton University Press, Princeton, NJ, 1963.
[9] S. Smale, Bull. Am. Math. Soc. 73 (1967) 747–817.
[10] T. Matsumoto, L. Chua, M. Komuro, IEEE Trans. Circuits Syst. CAS 32 (1985) 797–818.
[11] M. Komuro, R. Tokunaga, T. Matsumoto, L. Chua, A. Hotta, Int. J. Bifurcat. Chaos 1 (1991) 139–182.